# Critical Point Coupling and Proximity Effects in $^4$He at the Superfluid Transition

Justin K. Perron* and Francis M. Gasparini†

*Department of Physics, University at Buffalo, The State University of New York, Buffalo, New York 14260, USA*

(Received 11 January 2012; published 18 July 2012)

We report measurements of the superfluid fraction $\rho_s/\rho$ and specific heat $c_p$ near the superfluid transition of $^4$He when confined in an array of $(2\ \mu\text{m})^3$ boxes at a separation of $S = 2\ \mu$m and coupled through a 32.5 nm film. We find that $c_p$ is strongly enhanced when compared with data where coupling is not present. An analysis of this excess signal shows that it is proportional to the finite-size correlation length in the boxes $\xi(t, L)$, and it is measurable as far as $S/\xi \sim 30 - 50$. We obtain $\xi(0, L)$ and the scaling function (within a constant) for $\xi(t, L)$ in an $L^3$ box geometry. Furthermore, we find that $\rho_s/\rho$ of the film persists a full decade closer to the bulk transition temperature $T_\lambda$ than a film uninfluenced by proximity effects. This excess in $\rho_s/\rho$ is measurable even when $S/\xi > 100$, which cannot be understood on the basis of mean field theory.

DOI: 10.1103/PhysRevLett.109.035302 PACS numbers: 67.25.dr, 64.60.an, 71.45.Gm, 74.45.+c

With low temperature superconductors, coupling and proximity effects are manifest on the scale of the zero-temperature correlation length $\xi_o$. This leads to the familiar Josephson effects in weak-link junctions and proximity effects at a superconductor-normal metal interface [1]. One might suppose that in $^4$He near the superfluid transition temperature $T_\lambda$ analogous effects would occur on the scale of the temperature-dependent bulk correlation length $\xi(t)$ where $t = |1 - T/T_\lambda|$. Indeed, Josephson effects have been measured between bulk superfluids separated by weak links of dimensions $\sim\xi(t)$ [2,3]. However, recent measurements with arrays of $^4$He dots have demonstrated that proximity effects exist over a much larger scale [4]. Here we report measurements which quantify both proximity and coupling. To see both of these effects, one must arrange for helium to be confined in contiguous regions with different superfluid transition temperatures. In our case, this is an array of $L^3$ boxes separated by and linked through a uniform thin film. We vary the coupling between boxes by changing their separation. At large separation, the helium in the boxes will behave as isolated dots, while at very small separation and, hence, large coupling, the array will behave like a two dimensional film of thickness $L$. The thin film in equilibrium with the boxes will be influenced by the boxes both in its specific heat and its superfluid density. This influence will be present even in the limit of large separation of the boxes when the coupling among them is very small. Thus, even though the boxes-film system should be considered together as a single thermodynamic system, these effects can be separated and identified.

Surprisingly, the observed effects are manifest at distances much larger than $\xi(t)$. When one considers that this system is finite and the divergence of $\xi(t)$ is not physically possible, this becomes even more surprising. Indeed, in this system $\xi(t)$ must deviate from the bulk behavior to some finite-size correlation length $\xi(t, L)$ which must round off to a value $\lesssim L$. Our work shows that the observed effects, although existing over distances many times $\xi(t, L)$, are governed by $\xi(t, L)$. We note that $\xi(t, L)$, just like all of the thermodynamic responses near the transition, can be described by a scaling function $f$ such that $\xi(t, L) = \xi(t, \infty) f(L/\xi(t, \infty))$ [5], or equivalently $\xi(t, L) = LX(t(L/\xi_0)^{1/\nu})$ [6]. The latter form is perhaps more intuitive because at $t = 0$, $\xi(0, L) = LX(0)$ with $X(0) \leq 1$, since $\xi(t, L)$ cannot become larger than $L$. In contrast to low temperature superconductors, we believe the long range effect is a reflection of the role of critical fluctuations. Thus, these coupling-proximity effects are new phenomena which should also be manifest in other systems, such as magnets at the critical point.

Measurements reported in this Letter are made on $^4$He confined in an array of 69 million $(2\ \mu\text{m})^3$ boxes spaced $2\ \mu$m edge-to-edge and connected through a $32.5 \pm 1.2$ nm thick film (see Fig. 1). The film extends along the perimeter of the cell beyond the limits of the array of

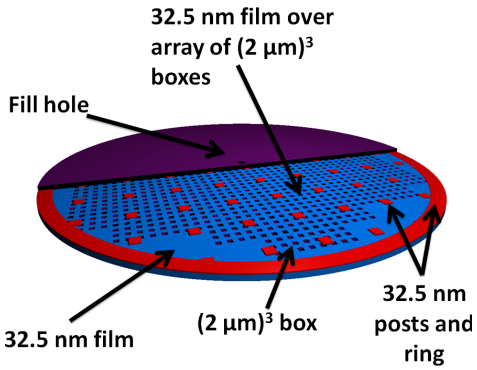


FIG. 1 (color online). Schematic rendering, not to scale, of the confinement cell. The cell is formed with two 50 mm diameter silicon wafers bonded at a separation determined by the 32.5 nm posts and ring. This oxide pattern is formed on the top wafer. The bottom wafer has an array of $(2\ \mu\text{m})^3$ boxes at $2\ \mu$m separation.

 

boxes. Thus, within the same cell, three different thermodynamic systems can be identified: an isolated 32.5 nm uniform film, a 32.5 nm film in contact with an array of $(2\ \mu\text{m})^3$ boxes of $^4$He, and the $(2\ \mu\text{m})^3$ boxes of $^4$He coupled through the 32.5 nm film. This geometry is achieved with patterned $SiO_2$ on two directly bonded Si wafers [7]. Cells prepared this way can be examined for uniformity of spacing using interferometry in the infrared [7,8]. For the present cell, we expect that the separation in the film region will be within $\pm 1.2$ nm, which is the standard deviation in the measured oxide thickness after growth. The $(2\ \mu\text{m})^3$ boxes are formed in an oxide $2074 \pm 1.34$ nm thick. The etching process produces an opening of $2.00 \times 2.00\ \mu\text{m}^2$ with rounded vertical corners (see [8] for an image of similar boxes). The procedure for staging the cell on the cryostat has been described in previous work [9].

The heat capacity is measured using a modified [9] version of conventional ac calorimetry [10]. This technique involves maintaining an average cell temperature while imposing small temperature oscillations, typically a few $\mu$K in our case. The signal is averaged for several minutes thereby achieving a temperature resolution of $\sim$50 nK. This technique is used to measure the heat capacity of the entire cell, which includes contributions from the addenda (the silicon wafers, heat sinks, etc.) as well as the $^4$He in the boxes and in both film regions. To obtain the specific heat $c_p$ of the $^4$He in the boxes, the heat capacity of the empty cell is subtracted from the total heat capacity. A separate measurement of a cell with just a 33.6 nm planar film [11] allowed us to subtract the contribution of a uniform film, amounting to $\sim$3% of the total heat capacity. After performing these subtractions, and in the absence of coupling and proximity effects, one should be left with only the heat capacity of the $^4$He in the $(2\ \mu\text{m})^3$ boxes. This was converted to a specific heat by dividing by the number of moles in the boxes and further normalizing to the bulk $c_p$ above $T_\lambda$ for $t \gtrsim 3 \times 10^{-3}$. The result is shown in Fig. 2 as filled red circles. The data have two branches: the lower is for $T > T_\lambda$, the upper for $T < T_\lambda$. Also plotted are two sets of data taken for $(2\ \mu\text{m})^3$ confinement but with different connectivities. One array was connected through a 10 nm thick film in 2 $\mu$m long and 2 $\mu$m wide channels [12,13] and a second array, at 4 $\mu$m edge-to-edge, connected through a 31.7 nm film [4]. The agreement between these two sets of data leads us to conclude that the confinement for both of these arrays represent very nearly independent dots of helium in $(2\ \mu\text{m})^3$ volume [14]. When the current $(2\ \mu\text{m})^3$ data are compared with these earlier data, it is apparent that the present data are greatly enhanced. Thus, we conclude that these boxes do not act as isolated entities, but couple through a 32 nm film which is normal (see below) through most of this temperature region. The temperature range of this enhancement spans from $t \sim 1 \times 10^{-3}$ for $T < T_\lambda$ to $t \sim 3 \times 10^{-4}$ for $T > T_\lambda$.

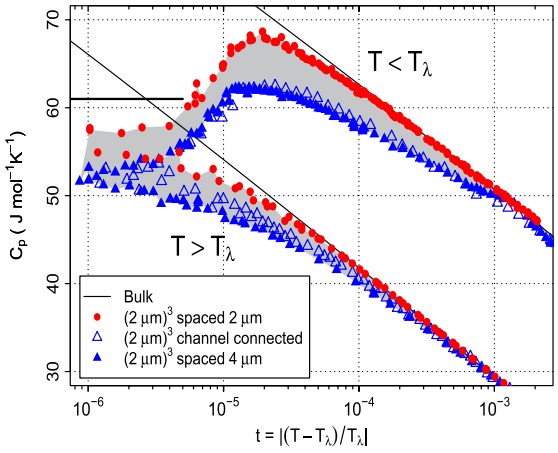


FIG. 2 (color online). The specific heat of $^4$He confined in $(2\ \mu\text{m})^3$ boxes with different connectivities as a function of reduced temperature $t$. The solid lines are the behavior of bulk helium. The data for the current cell, with boxes spaced 2 $\mu$m edge-to-edge show a large enhancement in $c_p$ relative to the other data sets. This is indicated by the shaded region.

For the bulk correlation length, one has $\xi(t) = \xi_o t^{-\nu}$, with $\nu = 0.6705$ [15], $\xi_o^+ = 0.143$ nm, and $\xi_o^- = 0.352$ nm for above and below $T_\lambda$, respectively. Thus, the enhancement in the specific heat $\delta c_p$ (the shaded region) is measurable when $S/\xi(t) \sim 30 \rightarrow 50$, with $S = 2\ \mu$m, the edge-to-edge spacing of the boxes.

The importance of the correlation length is made evident in Fig. 3. This is a log-log plot of $\delta c_p$ vs $t$. The open circles are for $T > T_\lambda$, the filled circles are for $T < T_\lambda$. There is a region in this plot, for larger $t$'s and $T > T_\lambda$, that is consistent with the same power law as $\xi(t)$, i.e., the solid lines with a $t^{-\nu}$ dependence. This indicates that in this region $\delta c_p \propto \xi(t)$. The power law for $\delta c_p$ rolls off for small $t$ as

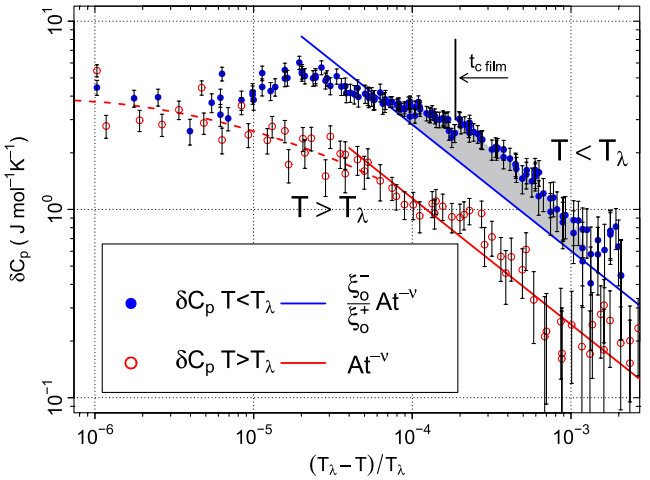


FIG. 3 (color online). The enhancement of the specific heat on a log-log scale. The solid lines have the same temperature dependence of $\xi(t)$ (see text for details). The dashed line is a guide to the eye.

one might expect from the earlier discussion of finite-size effects on $\xi(t)$. Specifically, if one assumes that $\delta c_p$ is proportional to $\xi(t, L)$, then for large $t$ one expects $\delta c_p \propto \xi(t, L) \simeq \xi(t)$. While for small $t$, $\xi(t, L)$ must roll off to a constant which is expected to be less than $L$. This finite-size behavior of the correlation length for a confined system is described by the scaling function $X$ introduced earlier. Assuming $\delta c_p \propto \xi(t, L)$, one can use Fig. 3 to evaluate $\xi(0, L) \simeq \xi(10^{-6}, L)$,

$$\xi(0, L) \simeq \frac{\xi(t = 10^{-4}, L = \infty)\delta c_p(t = 10^{-6})}{\delta c_p(t = 10^{-4})}. \quad (1)$$

This yields $\xi(0, L)/L = 0.14 \pm 0.02$. A similar analysis for $\delta c_p$ can be carried out for the helium confined in $(1\ \mu\text{m})^3$ boxes (see Fig. 5 in [4]). It should be noted that with no data available for isolated $(1\ \mu\text{m})^3$ boxes, $\delta c_p$ was deduced using finite-size scaling as discussed in [4]. The $(1\ \mu\text{m})^3$ data show a very similar behavior to the $(2\ \mu\text{m})^3$ data for $T > T_\lambda$. There is a region for $t \gtrsim 10^{-4}$ consistent with the $t^{-\nu}$ dependence of the bulk correlation length and a roll off for smaller $t$. Using Eq. (1) with these data, we obtain $\xi(t = 0, L)/L = 0.13 \pm 0.04$. These results are consistent for two different values of $L$. This ratio is $X(0)$, the value of the scaling function for a box geometry at $T_\lambda$. Also, the locus of $\delta c_p$ for $T > T_\lambda$ shown in Fig. 3 can be identified with $X(t(L/\xi_0)^{1/\nu})$ within a multiplicative constant which must depend on the strength of coupling between the boxes. We are unaware of any experimental results for $\xi(t = 0, L)$ or $X(t(L/\xi)^{1/\nu})$ in other critical systems. Furthermore, we are not aware of any calculations of $X$ appropriate for our case, but it is interesting to note that, although not strictly applicable, for 2D Ising strips of width $L$ and the energy-energy correlation length, one has $\xi(t = 0, L)/L = 1/2\pi \simeq 0.16$ [16].

Continuing with Fig. 3, the rise in $\delta c_p$ for $T < T_\lambda$ indicates that $\xi(t, L)$ continues to increase reaching a maximum of $\sim 0.20 \times L$ near $t \simeq 2 \times 10^{-5}$, where the heat capacity is also maximum. Below this region the data do not follow a power law as indicated by the top straight line drawn at $\xi_o^-/\xi_o^+ = 2.46$. There is a reason for this behavior. Recall that the data have been analyzed by subtracting from the measured heat capacity the expected contribution of a uniform film uninfluenced by the presence of the boxes. Thus, the shaded "bubble" in the data for $\delta c_p$ represents the extra contribution to the film's heat capacity near its own maximum due to the influence of the boxes. This will be more evident after we discuss the superfluid density data. Equivalently, one could also say that this is the enhancement in the collective behavior of the boxes-film system in the region where the film orders.

The superfluid fraction $\rho_s/\rho$ is determined using adiabatic fountain resonance [17]. This involves imposing a small temperature oscillation on the cell over a range of frequencies, thus exciting a resonant superfluid flow between the filling line and the cell. With the current cell design we were able to observe more than one resonance: one, a strong resonance associated with the region of the film outside the array of $(2\ \mu\text{m})^3$ boxes that persisted to $t \sim 3 \times 10^{-3}$, as well as a second, weaker resonance associated with the $^4$He film above the array of boxes. This persisted to $t \sim 2 \times 10^{-4}$.

The $\rho_s/\rho$ data are shown in Fig. 4. Also plotted are $\rho_s/\rho$ data from two previous cells: a 33.6 nm film uninfluenced by any boxes [11] and a 31.7 nm film over an array of $(2\ \mu\text{m})^3$ boxes separated at 4 $\mu$m edge to edge [4], twice the separation in the present cell. All of these data are for what we consider the same thickness films—within the measured uncertainty of the oxide thickness—but different proximity effects. The open circles are data for the fully planar film—with no proximity effects. They agree with data from other planar films of thickness $d$ [8] in their expected value of $t_c(d) \simeq 0.003$, as well as the magnitude of $\rho_s/\rho$ at $t_c$ relative to the expected Kosterlitz-Thouless jump [18], the horizontal line in Fig. 4. This is given by $\Delta\rho_s = 4m/d\lambda_T^2$, where $\lambda_T$ is the thermal wavelength at $T = T_c$, and $m$ is the $^4$He mass. The data overlapping these (the filled circles) come from the present cell. We interpret these as coming from the border region (see Fig. 1), where indeed the film is uniform and uninfluenced by the boxes. The overlap of these two sets of data from two different cells in separate experiments is strong confirmation of our interpretation.

The remaining two sets of data in Fig. 4 show the remarkable effect due to the influence of the helium in the boxes on the film in equilibrium with them. When the boxes are at 4 $\mu$m separation (the open triangles), the intervening film is shifted in $t_c$ by about 0.001, $\rho_s/\rho$ persists to a lower value than the predicted KT jump, and one can see an overall enhancement in $\rho_s/\rho$ far below $t_c$ [4]. An even more remarkable behavior is seen for the film data when the boxes are at 2 $\mu$m separation

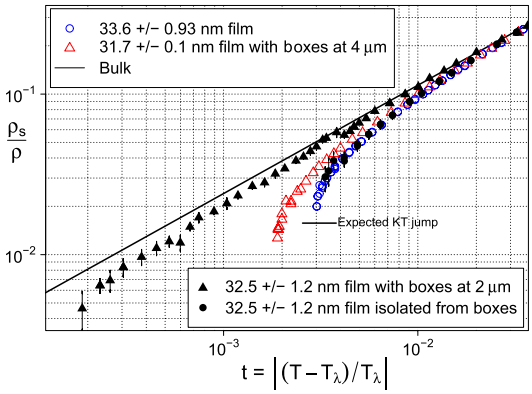


FIG. 4 (color online). The superfluid fraction $\rho_s/\rho$ for $^4$He films with the same nominal thickness of 32 nm. Two sets (filled and open circles) represent isolated films, the other sets (filled and open triangles) are films influenced by $(2\ \mu\text{m})^3$ boxes (see text for details). The solid line represents bulk helium.

(filled triangles). Here $\rho_s/\rho$ persists a full decade closer to $T_\lambda$, and the enhancement of $\rho_s/\rho$ is even larger. For these data, we note that the vanishing of $\rho_s/\rho$ is near $t_c \sim 2 \times 10^{-4}$ (see Fig. 3). This reinforces our earlier interpretation of the "bubble" in Fig. 3 as an enhancement of the film's specific heat due to coupling to the boxes. The coincidence of these two independent measurements is a strong argument for this interpretation.

A way to appreciate how unexpected these results are is to consider the influence of bulk helium adjoining helium confined in a slit (a film). This was done by Mamaladze and Cheishvili [19,20] using what has been called $\Psi$ theory [21]. This is a mean field theory with modified exponents to reflect more closely the critical behavior of $^4$He. We have now evaluated $\rho_s/\rho$ for the geometry of bulk-(weak link film)-bulk, thus mimicking our box-film-box situation. This calculation shows that for a 32 nm film and 4 or 2 $\mu$m separation there should be no measurable enhancement of $\rho_s/\rho$. In fact, for a film 32 nm thick and only 64 nm long separating bulk regions of helium, the effect on $\rho_s/\rho$ of the film is much smaller than what we see at micrometers separation. It is clear one cannot understand our data from a mean field approach which, by implication, suggests that critical fluctuations must be important. In helium, the bulk correlation length for $T < T_\lambda$ is $\xi^-(t) = (0.352\ \text{nm})t^{-\nu}$ and varies between 0.17 and 0.007 $\mu$m in the region where we observe an enhancement in the superfluid fraction. This length, as remarked before for the specific heat, is much smaller than the separation of the boxes. So while it seems evident that fluctuations are important, their influence is felt over a much larger scale than $\xi(t)$ and, therefore, even more so for $\xi(t, L)$. This is very surprising since the correlation length at a continuous transition is understood as "the distance to which order propagates" [22] or "the distance over which information is transferred" [23]. One is forced to ask how the neighboring boxes have information about each other. This remains an open question.

Our measurements are a systematic investigation of proximity and coupling effects in liquid $^4$He, which convincingly show, despite extending over distances much farther than $\xi(t, L)$, that $\xi(t, L)$ is the relevant parameter in these effects. This implies the relevance of critical fluctuations and leads us to believe similar effects should be observable in other critical systems near a continuous transition. Indeed, analogous long range effects have already been observed in high temperature cuprate superconductors [24,25].

This work was supported by the NSF Grants No. DMR-0605716 and No. DMR-1101189, The Cornell Nanoscale Science and Technology Facility Project number 526-94, The Mark Diamond Research Fund of the University at Buffalo, and internal university funding. The authors are also indebted to the University at Buffalo's College of Arts and Sciences Instrument Shop.

*perronjk@gmail.com
†fmg@buffalo.com

[1] See, for example, M. Tinkham, *Introduction to Superconductivity* (McGraw-Hill, New York, 1996).
[2] K. Sukhatme, Y. Mukharsky, T. Chui, and D. Pearson, Nature (London) **411**, 280 (2001).
[3] E. Hoskinson, Y. Sato, and R. E. Packard, Phys. Rev. B **74**, 100509 (2006).
[4] J. K. Perron, M. O. Kimball, K. P. Mooney, and F. M. Gasparini, Nature Phys. **6**, 499 (2010).
[5] E. Brezin, J. Phys. (Paris) **43**, 15 (1982).
[6] V. Privman and M. E. Fisher, Phys. Rev. B **30**, 322 (1984).
[7] I. Rhee, D. J. Bishop, A. Petrou, and F. M. Gasparini, Rev. Sci. Instrum. **61**, 1528 (1990).
[8] F. M. Gasparini, M. O. Kimball, K. P. Mooney, and M. Diaz-Avila, Rev. Mod. Phys. **80**, 1009 (2008).
[9] S. Mehta and F. M. Gasparini, J. Low Temp. Phys. **110**, 287 (1998).
[10] P. F. Sullivan and G. Seidel, Phys. Rev. **173**, 679 (1968).
[11] J. K. Perron and F. M. Gasparini, J. Phys. Conf. Ser. (to be published).
[12] K. P. Mooney, Ph.D. thesis, University at Buffalo, SUNY, 2006.
[13] J. K. Perron, M. O. Kimball, K. P. Mooney, and F. M. Gasparini, J. Phys. Conf. Ser. **150**, 032082 (2009).
[14] We note that for one of the measurements the 31.7 nm film adds a small structure to the data which is significant and is described in [4]. This is barely visible in Fig. 2 and outside the relevant temperature region.
[15] L. S. Goldner and G. Ahlers, Phys. Rev. B **45**, 13129 (1992).
[16] V. Privman, P. C. Hohenberg, and A. Aharony, in *Phase Transitions and Critical Phenomena*, edited by C. Domb and J. L. Lebowitz (Academic Press, New York, 1991), Vol. 14.
[17] F. M. Gasparini, M. O. Kimball, and S. Mehta, J. Low Temp. Phys. **125**, 215 (2001).
[18] D. R. Nelson and J. M. Kosterlitz, Phys. Rev. Lett. **39**, 1201 (1977).
[19] Y. G. Mamaladze and O. D. Cheishvili, Sov. Phys. JETP **23**, 112 (1967).
[20] L. V. Kiknadze, Y. G. Mamaladze, and O. D. Cheishvili, Izmeritel'naya Tekhnika **7**, 29 (1984); Meas. Tech. **27**, 605 (1984).
[21] V. L. Ginzburg and A. A. Sobyanin, J. Low Temp. Phys. **49**, 507 (1982).
[22] M. E. Fisher, in *Proceedings of the International School of Physics*, edited by M. S. Green (Academic Press, New York, 1971).
[23] L. P. Kadanoff, *Statistical Physics: Statics, Dynamics and Renormalization* (World Scientific Publishing, Singapore, 2000), p. 232.
[24] I. Bozovic, G. Logvenov, M. A. J. Verhoeven, P. Caputo, E. Goldobin, and M. R. Beasley, Phys. Rev. Lett. **93**, 157002 (2004).
[25] E. Morenzoni, B. M. Wojek, A. Suter, T. Prokscha, G. Logvenov, and I. Bozovic, Nature Commun. **2**, 272 (2011).